Received: 30 September 2016 | Revised: 31 March 2017 | Accepted: 13 April 2017

DOI: 10.1002/mc.22664

RESEARCH ARTICLE

WILEY Molecular Carcinogenesis

Copy number variation, increased gene expression, and molecular mechanisms of neurofascin in lung cancer

Johanna Samulin Erdem | Yke Jildouw Arnoldussen | Vidar Skaug | Aage Haugen | Shanbeh Zienolddiny

Department of Chemical and Biological Work Environment, National Institute of Occupational Health, Oslo, Norway

Correspondence
Shanbeh Zienolddiny, Department of Chemical and Biological Work Environment, National Institute of Occupational Health, Oslo NO-0363, Norway.
Email: shan.zienolddiny@stami.no

Funding information
Norwegian Cancer Society

Metastasis and cell adhesion are key aspects of cancer progression. Neurofascin (NFASC) is a member of the immunoglobulin superfamily of adhesion molecules and, while studies on NFASC are inadequate, other members have been indicated pivotal roles in cancer progression and metastasis. This study aimed at increasing the knowledge on the involvement of adhesion molecules in lung cancer progression by studying the regulation and role of NFASC in non-small cell lung cancer (NSCLC). Here, copy number variations in the *NFASC* gene were analyzed in tumor and non-tumorous lung tissues of 204 NSCLC patients. Frequent gene amplifications (OR = 4.50, 95%CI: 2.27-8.92, $P \leq 0.001$) and increased expression of NFASC ($P = 0.034$) were identified in tumors of NSCLC patients. Furthermore, molecular mechanisms of NFASC in lung cancer progression were evaluated by investigating the effects of NFASC silencing on cell proliferation, viability, migration, and invasion using siRNA technology in four NSCLC cell lines. Silencing of NFASC did not affect cell proliferation or viability but rather decreased NSCLC cell migration ($P \leq 0.001$) and led to morphological changes, rearrangements in the actin cytoskeleton and changes in F-actin networks in migrating NSCLC cell lines. This study is the first to report frequent copy number gain and increased expression of NFASC in NSCLC. Moreover, these data suggest that NFASC is a novel regulator of NSCLC cell motility and support a role of NFASC in the regulation of NSCLC progression.

KEYWORDS
cancer progression, cell adhesion molecule, CNV, NFASC, non-small cell lung cancer

1 | INTRODUCTION

Neurofascin (NFASC) belongs to the L1 family of cell adhesion molecules (L1CAMs). This family includes three additional structurally related transmembrane proteins; L1 cell adhesion molecule (L1 also known as L1CAM), cell adhesion molecule L1 like (CHL1), and neuronal cell adhesion molecule (NrCAM). NFASC is a heavy glycosylated multi-domain protein, which contains an ectodomain with six Ig-like domains and up to five fibronectin-type III domains, a single pass transmembrane PAT region and a short cytoplasmic domain. Alternative splicing produces structural diversity of the NFASC polypeptides and four major forms of 186, 180, 166, and 155 kDA have been described.[1] NFASC interacts with many different cellular proteins. Extracellularly, NFASC binds integrins, proteoglycans, and other CAMs to potentiate cell motility and signal transduction. Intracellularly, the cytoplasmic tail binds to the actin cytoskeleton through ankyrin allowing for mediation of intracellular signal transduction and regulation of cell motility.[2] NFASC has been studied extensively in the brain, where it serves as a

Abbreviations: AKT1, V-Akt murine thymoma viral oncogene homolog 1; CDKN1C, cyclin dependent kinase inhibitor 1C; CHL1, cell adhesion molecule L1 like; CI, confidence interval; CNVs, copy number variations; CSF3, colony stimulating factor 3; DUSP6, dual specificity phosphatase 6; ERK, extracellular signal-regulated kinase; FHIT, fragile histidine triad; FTH1, ferritin heavy chain 1; GAPDH, glyceraldehyde-3-phosphate dehydrogenase; KRAS, KRAS proto-oncogene, GTPase; KRT14, keratin 14; L1, L1 cell adhesion molecule; L1CAMs, L1 family of cell adhesion molecules; MAPK, mitogen-activated protein kinase; MKI67, marker of proliferation Ki-67; MMP, matrix metalloproteinase; NFASC, neurofascin; NFKB, nuclear factor kappa B; NrCAM, neuronal cell adhesion molecule; NSCLC, non-small cell lung cancer; OR, odds ratio; PVDF, polyvinylidene difluoride; qPCR, quantitative real-time PCR; RASSF1, Ras association domain family member 1; STAT, signal transducer and activator of transcription; TBST, Tris-buffered saline—Tween-20; TERT, telomerase reverse transcriptase.

switch between neuronal plasticity and stability by linking the cytoskeleton and the extracellular matrix.[1] However, NFASC is also expressed in several other organs including lung.

Copy number variations (CNVs) and consequent alterations in gene expression patterns are involved in the development and progression of human malignancies. In breast cancer, *L1* copy number gain has been reported to correlate with increased L1 gene expression.[3] Similarly, *CHL1* copy number deletion and decreased gene expression have been reported in breast cancer patients.[4,5] L1 expression is upregulated in a variety of tumor types including NSCLC, glioma, ovarian, pancreatic, gastric, and colon carcinomas; however, the presence of *L1* CNVs in these cancers has not been investigated.[6–12]

Changes in the expression of the *L1CAM* genes have been reported to affect tumor progression and metastasis.[13–15] The L1 protein mediates cell-cell binding in the absence of E-cadherin and cell-cell cohesion in invading melanoma and colorectal carcinoma.[16] L1 is present mainly at the invasive front and not the tumor mass of colon cancers and induces expression of metastasis-associated genes in fibroblast cells.[7,17] L1 disrupts adherent junctions and both L1 and CHL1 regulate the motility of breast cancer cells.[5,18] Moreover, soluble L1 produced by proteolytic cleavage of membrane-bound L1 may act as a chemoattractant for breast cancer cells.[19] L1 is also required for the growth and survival of glioma stem cells, suggesting that L1 might have a role not only in cancer invasiveness but also in cancer cell survival.[20] Altogether, these findings have made L1 an interesting biomarker and prognostic tool in patients with epithelial ovarian carcinoma and colorectal cancer.[8,11,21] L1 is also a target for chemosensitization as L1-interfering antibodies can be utilized to increase the therapeutic response of pancreatic and ovarian carcinomas.[22] Moreover, a role of NrCAM and CHL1 has been suggested in melanoma, glioblastoma, thyroid, and colon carcinomas.[23–26]

While adhesion molecules are important in cancer progression and metastasis, the role of L1CAM proteins in lung cancer is largely unknown. Here, we investigated CNVs in the *NFASC* gene and its expression in NSCLC. Furthermore, we studied mechanisms by which NFASC may affect lung cancer progression, by investigating lung cancer cell proliferation, adhesion, migration, and invasion *in vitro*.

2 | MATERIAL AND METHODS

2.1 | Cases

Early-stage lung cancer patients (n = 204) were Caucasians of Norwegian origin admitted to Haukeland University Hospital in Bergen between 1988 and 1994, for primary surgery. The patients were enrolled in the study whenever practically feasible and informed written consent was given prior to surgery. The characteristics of the patients included in the study are summarized in Supplementary Table S1. Samples of adjacent non-tumorous lung tissue, confirmed by histology, were cut from the lobectomi specimens at the time of surgery. Tumor histology was confirmed by an experienced pathologist and samples containing ≥80% of tumor cells were included in the study. After resection, tumor and non-tumorous tissues were snap-frozen in liquid nitrogen and kept at −80°C until further processing. Lung cancer-related survival was available for 188 patients. Patients who died from other causes than lung cancer were censored. The study was approved by the Regional Committee for Medical and Health Research Ethics in South Norway in accordance with the WMA Declaration of Helsinki.

2.2 | Copy number analyses by quantitative PCR

DNA was extracted from frozen lung tissue samples using standard proteinase K digestion followed by phenol-chloroform extraction and ethanol precipitation. *NFASC* CNVs were evaluated by quantitative real-time PCR (qPCR) using SYBR Green I technology on an ABI PRISM® 7900HT Fast PCR System (Applied Biosystems, ThermoFisher Scientific, Waltham, MA), as previously described.[27] The multicopy gene *FTH1* was used as reference gene. Primer sequences are listed in Supplementary Table S2. Copy numbers below 1.5 and above 2.5 were defined as deleted and amplified, respectively.

2.3 | Cell culture and RNA silencing

Lung cancer cell lines H838, H460, H23, and H1435 were obtained from American Type Culture Collection (Rockville, MD) and authenticated in 2011 using DNA fingerprinting (Deutsche Sammlung von Mikroorganismen und Zellkulturen, Braunschweig, Germany). Cells were maintained in RPMI-1640 medium (ThermoFisher Scientific) with 10% FCS (ThermoFisher Scientific) and penicillin/streptomycin (Biowest SAS, Nuaillé, France) in 5% CO_2 at 37°C. Cells were passaged every 2nd or 3rd day. RNA silencing experiments were conducted in penicillin/streptomycin free medium in 6-well plates. The cells were seeded at the following concentrations: H838, 2.0E^5 cells/well; H460, 3.0E^5 cells/well; H23, 6.0E^5 cells/well; and H1435, 1.5E^6 cells/well. siRNA targeting human *NFASC* and non-target control were purchased from Applied Biosystems (ThermoFisher Scientific). Transfections were performed 24 h after seeding using 10 nM siRNA and Lipofectamin RNAiMAX reagent (Invitrogen, ThermoFisher Scientific) according to manufacturer's instructions. After 48 h the cells were used for functional analysis or harvested for analysis of RNA. Protein was extracted 72 h after transfection.

2.4 | Gene expression and gene ontology analysis

Total RNA was isolated from cells and lung tissue samples using PerfectPure RNA Cultured Cell Kit (5 Prime, Hilden, Germany) or standard Trizol extraction. RNA quality was assessed by 2100 Bioanalyzer (Agilent Technologies, Santa Clara, CA). Gene regulation following NFASC silencing was assessed using RT^2 First Strand cDNA Kit and RT^2 Profiler Lung Cancer Array (Qiagen, Hilden, Germany). Fold change and P values of NFASC silenced cells compared with controls were obtained from the ΔΔCT method using the GeneGlobe Data Analysis Center (Qiagen). For single gene expression analysis, total RNA was reverse transcribed using qScript cDNA synthesis (Quanta BioSciences, Beverly, MA). Gene expression was analyzed by qPCR using SYBR Green I technology. *GAPDH* was used as reference gene. CT values >33 were set as non-detectable in further analyses. ABI PRISM® 7900HT Fast or StepOnePlus Real-Time PCR Systems (Applied

Biosystems, ThermoFisher Scientific) were used in the analysis. Primer sequences are listed in Supplementary Table S2 and their specificity was determined by melting point analysis. Heat map and hierarchical clustering analysis of gene expression data were performed using the ComplexHeatmap package version 1.10.2 in R version 3.3.3. Gene ontology analysis was performed using Panther version 11.1.

2.5 | Western blotting

Total protein lysates were extracted from NFASC silenced and control cells using Mammalian Cell & Tissue Extraction kit (BioVision, Milpitas, CA) and membrane fractions were isolated using Mem-PER™ Plus Membrane Protein Extraction Kit (ThermoFisher Scientific). Concentrations were determined by Reducing Agent Compatible BCA Protein Assay kit (Biovision). Total protein lysates (80 μg) or membrane fractions (15 μg) were separated by 10% or AnyKD gradient (Biorad, Hercules, CA) SDS-PAGE as appropriate and transferred to an Immobilon PVDF membrane (Millipore, Bedford, MA). To prevent non-specific background binding, the membranes were incubated with 5% non-fat milk in Tris-buffered saline with 0.05% Tween-20 (TBST) for 1 h at room temperature. Membranes were incubated with primary antibodies against p-AKT, AKT, p-ERK, ERK, p-STAT1, STAT1 p-STAT3, STAT3, (Cell Signaling Technology, Inc., Beverly, MA), NFASC (Origene, Rockville, MD), and GAPDH (Santa Cruz Biotechnology, Santa Cruz, CA) over night at 4°C. After washing three times with TBST, the membranes were incubated with HRP-conjugated secondary antibody (Cell Signaling Technology) for 1 h at room temperature and proteins visualized by SuperSignal West Pico Chemiluminescent Substrate (ThermoFisher Scientific).

2.6 | Proliferation and cell viability

Cell viability and cell count were analyzed 48 h after transfection using the Via1-Cassette on the NucleoView NC-200 (Chemometec, Allerod, Denmark). Moreover, proliferation of transfected H838 cells was monitored for 48 h by the live-cell imaging system IncuCyte ZOOM (Essen BioScience, Ann Arbor, MI).

2.7 | Migration and invasion assays

Transfected cells were seeded at the concentration of $3.0E^4$ cells/well for H838 and H460, and 4.0E4 cells/well for H23 cells on ImageLock 96-well plates (Essen BioScience), coated with 100 ng/μL matrigel (Corning, Corning, NY). Cells were allowed to attach and the following day a wound was made in the cell monolayer using the wound maker pin tool (Essen BioScience). For analysis of cell migration, cells were washed and fresh culture medium was added to the wells. Cell migration was monitored for 48 h for H838 and H23 cells and for 7 days for H460 cells by live-cell imaging using IncuCyte ZOOM (Essen BioScience). For analysis of cell invasion, the cultured wells were washed and coated with 8 μg/μL matrigel. Culture medium was added to the wells and cell invasion was monitored for 6 days. Analyses were performed in two or three independent experiments with eight replicates in each. As H1435 cells did not form a monolayer on matrigel they were not suitable for wound closure analysis of migration and invasion. Thus, to investigate alterations in H1435 motility the cells were seeded 48 h after transfection in 6-well plates coated with 100 ng/μL matrigel at $1.5E^5$ cells/well and allowed to spread for 48 h after seeding. Cell spreading was analyzed using the IncuCyte ZOOM software.

2.8 | Adhesion

For analysis of cell adhesion transfected H838 cells were seeded in serum free medium at the concentration of $5.0E^4$ cells/well in 96-well plates precoated with 30 μg/mL of laminin, fibronectin, or collagen. Cells were allowed to attach for 30 min. Unbound cells were removed by gentle washing and bound cells were fixated using concentrated methanol and stained by crystal violet. Cell adhesion was analyzed in the IncuCyte ZOOM imaging software (Essen BioScience).

2.9 | Immunofluorescence confocal microscopy

Transfected cells were seeded at concentrations of $9.0E^5$ H838 cells/well, $1.0E^6$ H460 cells/well, and $8.0E^5$ H23 cells/well on cover slips in 6-well plates. The following day two parallel wounds were made in the cell monolayer and cells were incubated for an additional 12 h for H838 and H23 cells, and 48 h for H460 cells. Transfected H1435 cells were seeded at a concentration of $1.5E^6$ cells/well on matrigel-coated cover slips (100 ng/uL) and incubated for 48 h. Cells were fixed in 4% paraformaldehyde for 20 min and permeabilized with 0.1% Triton X-100 in PBS for 5 min. Cover slips were blocked by incubation with 5% BSA in 0.1% PBS-Triton X-100 for 1 h at room temperature. Alexa Fluor® 647 Phalloidin (ThermoFisher Scientific) was used to stain F-actin for 20 min according to the manufacturer's instructions. Cells were counterstained with Hoechst (Sigma-Aldrich, St. Louis, MO) to visualize cell nuclei. Fluorescence was visualized using a pinhole confocal microscope (Zeiss, Oberkochen, Germany) and images were acquired using an AxioCam camera (Zeiss). Cells surrounding the scratches were investigated for differences in cell morphology and F-actin expression.

2.10 | Statistical analysis

Statistical analyses were carried out using IBM SPSS software version 22.0. Associations between copy number variation and lung cancer were estimated by odds ratios (ORs) and their 95% confidence intervals (CIs) from conditional logistic regression adjusted for age, gender, total pack-years, and tumor histology. Patients with insufficient information on age, sex, or smoke data were excluded from the final statistical analysis. Effects of clinicopathological data on gene status were assessed by Chi-square or Fisher's exact test for categorical variables and by nonparametric tests for ordinal variables. Cancer-free survival was obtained by Kaplan Meier analysis. Gene and protein expression data were analyzed using *T*-test, nonparametric Mann-Whitney test or Wilcoxon Rank test as appropriate. Migration and invasion patterns were analyzed using the NLME package version 3.1-128 in R version 3.3.1 by nonlinear mixed-effects model fit by maximum likelihood. The model: $D\ [1 - \exp(-B \times \text{hour} - C \times \text{hour}^2)]$ was used, where *B* indicates the cells migration and invasion rate, and *D* indicates the final asymptotic cell density in the wound. Several models were assessed for their goodness of fit and predictive power, and the *C*

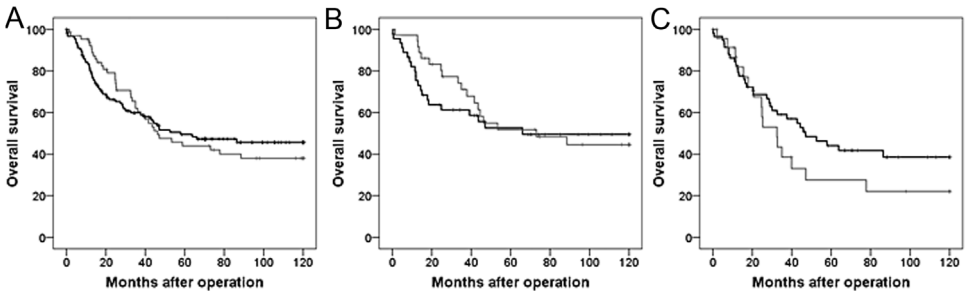

FIGURE 1 10-year survival of NSCLC patients with and without amplifications in the *NFASC* gene obtained from Kaplan-Meier Analysis. Black lines indicate patients with normal *NFASC* copy numbers, gray lines indicate patients with amplified *NFASC*. (A) Cancer-free survival of all NSCLC patients independent of histology. (B) Cancer-free survival in adenocarcinoma patients, $n = 82$. (C) Cancer-free survival in squamous cell carcinoma patients, $n = 83$

coefficient, a constant value, was added to give a closer fit between model predictions and data. For datasets where full wound closure was not reached, both *B* and *D* had treatment as fixed effect. In addition, nested random intercepts for treatment and well were added for *B* and *D*, allowing the rate and the asymptotic cell density to vary between replicates and experiments. For analysis of datasets where complete wound closure was reached, *B* was modeled identically as for the previous data, while *D* was set to 100 (Supplementary Fig. S1). $P \leq 0.05$ was considered significant.

3 | RESULTS

3.1 | Analysis of NFASC copy number variations in paired non-tumorous—tumor tissues

Analysis of CNVs in the *NFASC* gene demonstrated that NSCLC patients had a 4.5-fold higher odds of acquiring a copy number gain in DNA from tumor tissues than from adjacent non-tumorous tissues (OR: 4.50, 95%CI: 2.27-8.92, $P \leq 0.001$). Moreover, *NFASC* copy number loss was less frequent in tumor tissues than in non-tumorous tissues (OR: 0.28, 95%CI: 0.10-0.76, $P = 0.012$). Amplifications were more frequent in adenocarcinoma than in squamous cell carcinoma patients (47.2% vs 23.9%, $P = 0.016$). CNVs were not associated with gender, age, or smoking status of the patients (data not shown). Survival analysis suggested differences between histological subtypes on the cancer-free survival in patients with *NFASC* gene amplifications; however, these effects were not statistically significant (Fig. 1).

3.2 | Expression of NFASC in non-tumorous and tumor tissues from lung cancer patients

NFASC expression was analyzed in non-tumorous and tumor tissues from 159 patients. The expression level of NFASC was generally low in non-tumorous tissue and under detection level in 12.6% of the samples. Moreover, increased NFASC mRNA expression was more frequently observed in tumor tissues compared with non-tumorous tissues ($P = 0.034$).

3.3 | Silencing of NFASC *in vitro* and its effects on lung cancer pathways

Effects of NFASC silencing on lung carcinogenesis were identified using a pathway specific lung cancer array including 84 genes in the H838 cell line. This approach identified two clusters of differentially regulated genes as illustrated by hierarchical clustering and heat map analyses (Fig. 2A) following NFASC silencing in H838 cells (Fig. 2B). Gene ontology analysis showed that the differentially regulated genes in clusters 1 and 2 had binding, catalytic, structural, or transport activities. Moreover, the genes were involved in biological processes such as growth and development, organization of cell compartments, localization, and response to stimuli (Fig. 2C). In total nine genes were significantly regulated following NFASC silencing in H838 cells (Fig. 2D, Supplementary Table S3). The main effects were observed on colony stimulating factor 3 (CSF3) and dual specificity phosphatase 6 (DUSP6), which expressions were five- and twofold reduced following NFASC silencing in H838 cells. These genes regulate cellular events through mitogen-activated protein kinase (MAPK) 1 and 3 (commonly known as extracellular signal-regulated kinases, ERK1/2) and signal transducer and activator of transcriptions 1 and 3 (STAT1 and STAT3) signaling. Thus, the regulation of ERK1/2, STAT1, and STAT3 phosphoproteins was investigated in H838 cells. In addition, regulation of V-Akt murine thymoma viral oncogene homolog 1 phosphoprotein (p-AKT) was assessed. The levels of p-ERK1/2 and p-AKT were markedly reduced in NFASC silenced H838 cells compared to control cells (Fig. 3A,B). p-STAT1 and p-STAT3 levels were not affected by NFASC gene silencing in the H838 cell line.

The importance of NFASC in the identified pathways of lung carcinogenesis was further investigated by NFASC silencing in lung cancer cell lines representative of different lung cancer stages. Thus, effects of NFASC silencing on lung cancer cell growth, viability, and motility were investigated in H838 and H460 cells of metastatic origin as well as in the primary lung cancer cell lines H23 and H1435.

3.4 | Effects of NFASC silencing on the proliferation and viability of lung cancer cells

Effective NFASC silencing in H460, H23, and H1435 cells was demonstrated in Fig. 4A. NFASC silencing increased the expression of marker of proliferation Ki-67 (MKI67) in H838 (2.1-fold, $P = 0.004$) and H460 cells (1.7-fold, $P = 0.003$), but not in the primary lung cancer cells H23 and H1435 (Fig. 4B). However, NFASC silencing did not affect cell number nor viability in any of the analyzed cell lines (Supplementary Fig. S2).

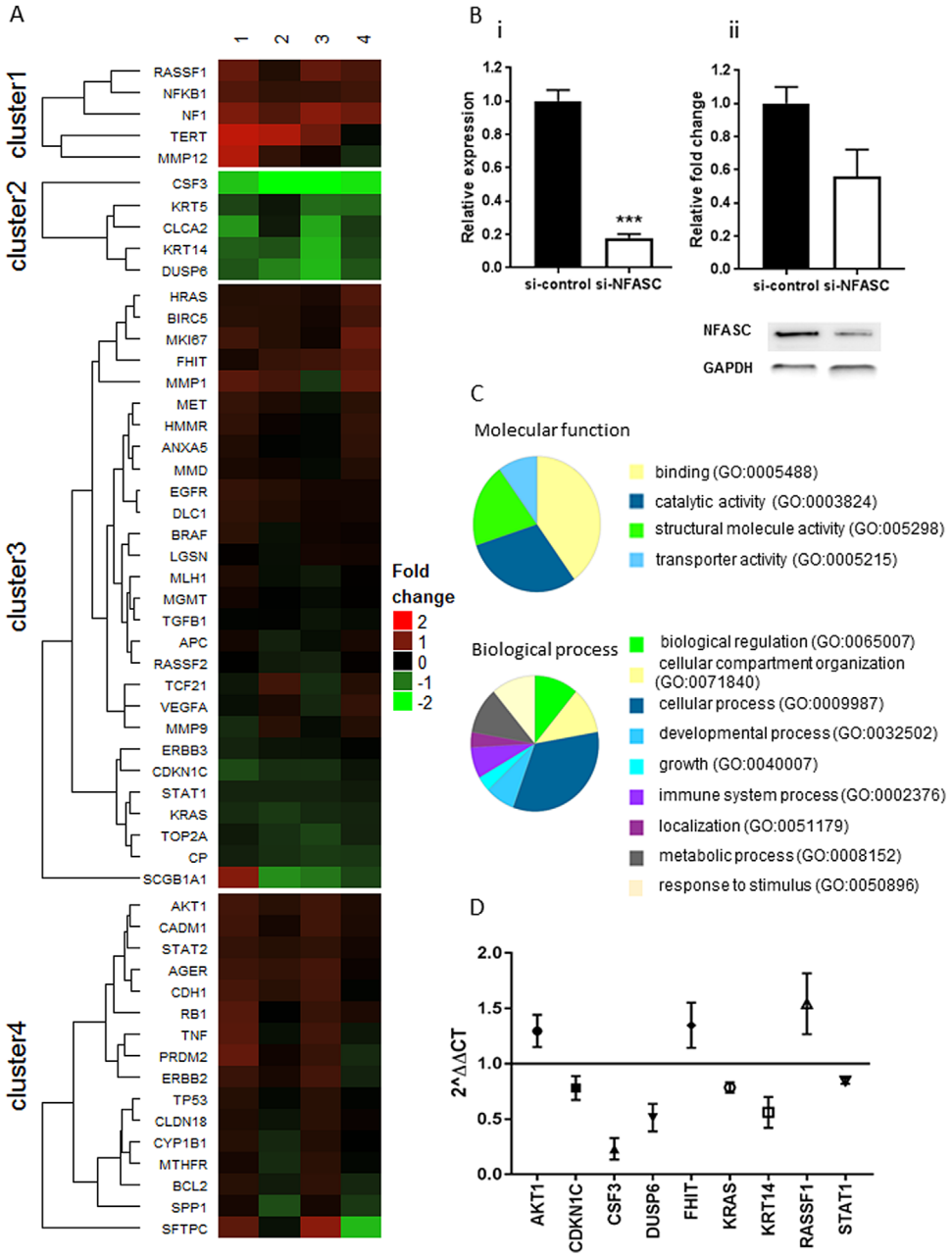

FIGURE 2 Effects of NFASC silencing on the expression of genes important in lung cancer was analyzed by the RT2 Profiler Lung Cancer Array in the H838 cell line. (A) Heat map and hierarchical clustering of gene expression in NFASC silenced H838 cells (si-NFASC). Values represent the $\log^2$ ratio over control cells (si-control). Each column represents a single si-NFASC replicate and each row represents a single gene. Expression levels are colored green for low intensities and red for high intensities. (B) Silencing of the NFASC gene in H838 cells: (i) NFASC gene expression; (ii) NFASC protein expression in si-control and si-NFASC cells 48 and 72 h after transfection, respectively. Bars represent mean ± SD, $n = 9$. ***$P \leq 0.001$ was obtained from nonparametric Mann-Whitney test. (C) Gene ontology analysis of differentially regulated genes (clusters 1 and 2). (D) Genes significantly regulated following NFASC silencing in H838 cells, values represent mean ± SD, $n = 6$

3.5 | Effects of NFASC silencing on lung cancer cell motility

NFASC silencing significantly decreased the motility of the four studied lung cancer cell lines. H838 cells had a decreased migration rate in NFASC silenced cells compared to controls ($P \leq 0.001$, Fig. 5A, B). Moreover, H838 NFASC silenced cells had a significantly lower invasion rate and overall invasion potential ($P \leq 0.001$) than control cells (Fig. 5C). Similarly, decreased migration potential or rate was observed in H460 and H23 NFASC silenced cells compared with controls ($P \leq 0.001$, Fig. 5D,E). However, these cell lines were not able to invade the matrigel and were not suitable for invasion analysis (data not shown). Furthermore, H1435 cells did not form monolayers on matrigel and could not be used in the wound healing assays. However, a clear difference in cell morphology and attachment or spreading was observed in the NFASC silenced H1435 cells compared with control

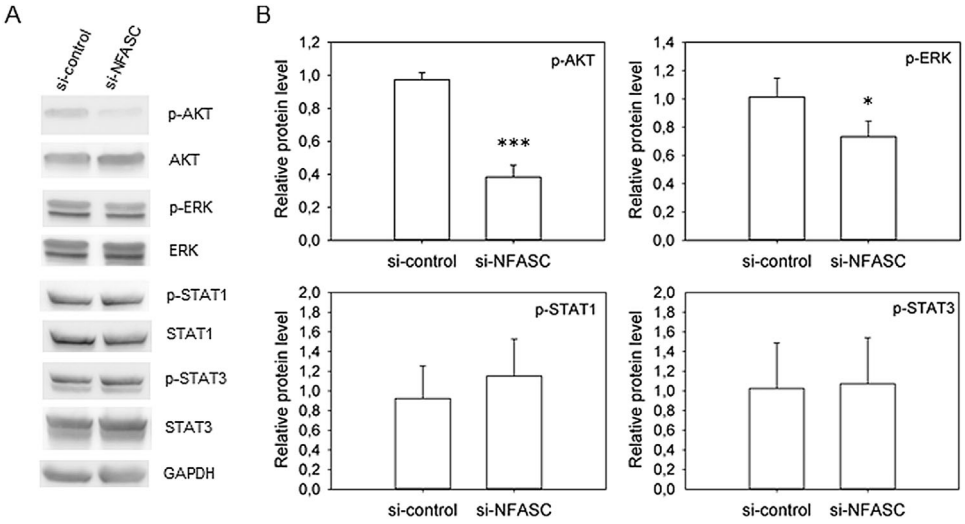

FIGURE 3 Phosphoprotein levels were altered in NFASC silenced H838 cells (si-NFASC) compared with control cells (si-control). (A) Cropped Western blot images are representative of data from three experiments. (B) Quantification of protein expression was performed by the Image J software. Bars represent mean ± SE, $n = 3$. $^{*}P \leq 0.05$ and $^{**}P \leq 0.01$ was obtained from *t*-test

cells. NFASC silenced H1435 cells were more densely clustered and showed less spreading than control cells 48 h after seeding on the matrigel surface (Fig. 5F). Finally, the effects of NFASC silencing on H838 cells' potential to adhere to different extracellular matrices were analyzed. Since H838 cells showed a very poor adhesion capacity to collagen 1, laminin, and fibronectin coatings were used for further analysis. NFASC silenced cells showed a reduced adhesion to both laminin ($P = 0.005$) and fibronectin ($P = 0.004$) compared to control cells after 30 min of incubation (Fig. 5G).

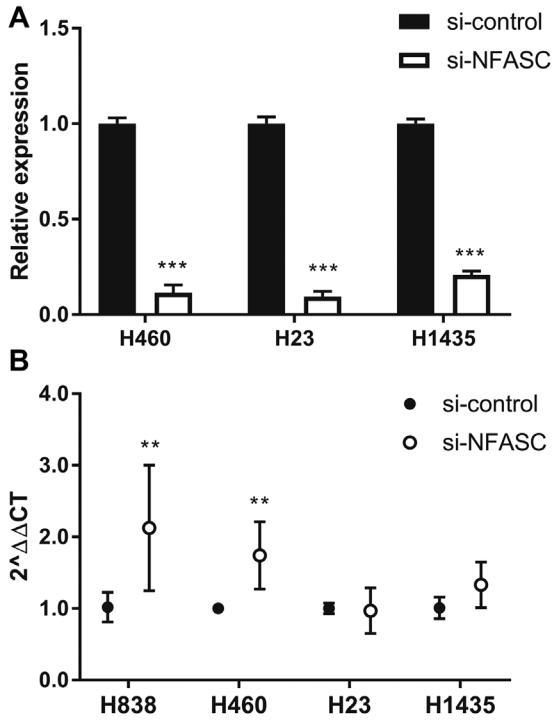

FIGURE 4 Effects of NFASC silencing on cell proliferation. (A) Silencing of the *NFASC* gene in H460, H23, and H1435 lung cancer cells. Bars represent mean ± SD, $n = 6$. (B) MKI67 expression was analyzed in NFASC silenced (si-NFASC) and control cells (si-control). Bars represent mean ± SD, $n = 6$. $^{***}P \leq 0.001$ and $^{**}P \leq 0.01$ were obtained from nonparametric Mann-Whitney test or *t*-test

3.6 | Effects of NFASC silencing on the organization of F-actin in migrating lung cancer cells

NFASC silencing altered the cytoskeletal organization of F-actin in migrating H838 cells (Fig. 6A). Cytoskeletal structures involved in cell migration, such as stress fibers and transverse arcs were observed in the majority of the control H838 cells (Fig. 6Ai-iii). In the NFASC silenced H838 cells a reorganization of F-actin was apparent (Fig. 6Aiv-vi). Fewer cells showed stress fibers and transverse arc formation, whereas the F-actin was more frequently arranged in the cortex of NFASC silenced H838 cells (Fig. 6Av-vi). Due to the slow migration rate of H460 cells, differences in cell morphology and F-actin organization were more subtle. However, throughout our experiments we observed a more pronounced F-actin staining in the migrating front of NFASC silenced H460 cells (Fig. 6B). Structural and morphological changes in migrating H23 and H1435 cells were also apparent following NFASC silencing. Migrating NFASC silenced H23 cells had fewer long cell protrusions than control cells (Fig. 6C). Moreover, H1435 cells were present in more dense clusters and found more often as individual cells following NFASC silencing. These clusters also showed stronger F-actin staining than H1435 control cells (Fig. 6D). Altogether, these data might indicate a role of NFASC in regulation of cell morphology and in rearrangement of F-actin important for cell motility, adhesion, locomotion, and migration.

4 | DISCUSSION

L1CAM family members L1, CHL1, and NrCAM have been annotated roles in cancer progression and metastasis, and are involved in the regulation of proliferation and migration of diverse cancer

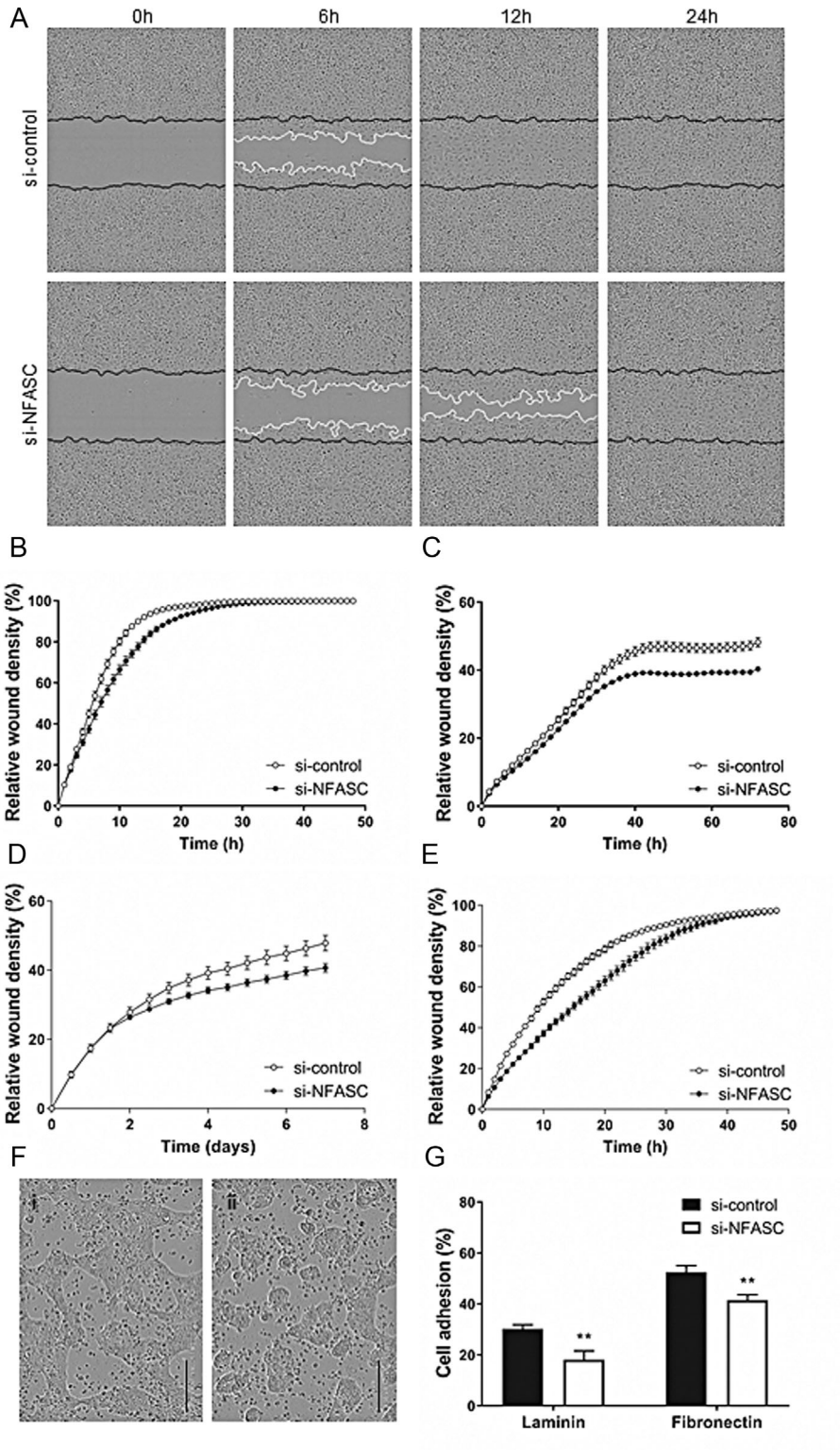

FIGURE 5 NFASC silencing altered the motility of NSCLC cells. NFASC was silenced using siRNA technology. Cell migration and invasion were analyzed using a wound healing assay by live-cell imaging on IncuCyte ZOOM. (A) Presented images of migrating H838 cells at selected time points are from one representative experiment. The inflicted wound front is highlighted in black and the migrating cell front is highlighted in white. (B-E) Cell migration and invasion of NFASC silenced (si-NFASC) and control cells (si-control) is illustrated as mean relative wound density ± SE. Relative wound density is the cell density in the wound area expressed relative to the cell density outside of the wound area over time. This metric normalizes for changes in cell density caused by proliferation. (B) H838 cell migration, and (C) invasion were monitored for 48 and 72 h, respectively. (D) H460 and (E) H23 cell migration were monitored for 7 days and 48 h, respectively. (F) NFASC silencing decreased H1435 cell spreading on matrigel surface, (i) si-control cells; (ii) si-NFASC cells 48 h after seeding. Scale bars indicate 200 µm. (G) NFASC silencing decreased H838 cells adhesion to laminin and fibronectin. Cell adhesion was assessed in si-control and si-NFASC cells after 30 min by crystal violet staining. Bars indicate mean ± SE, $n = 9$. $^{**}P \leq 0.01$ was obtained from nonparametric Mann-Whitney test or *t*-test

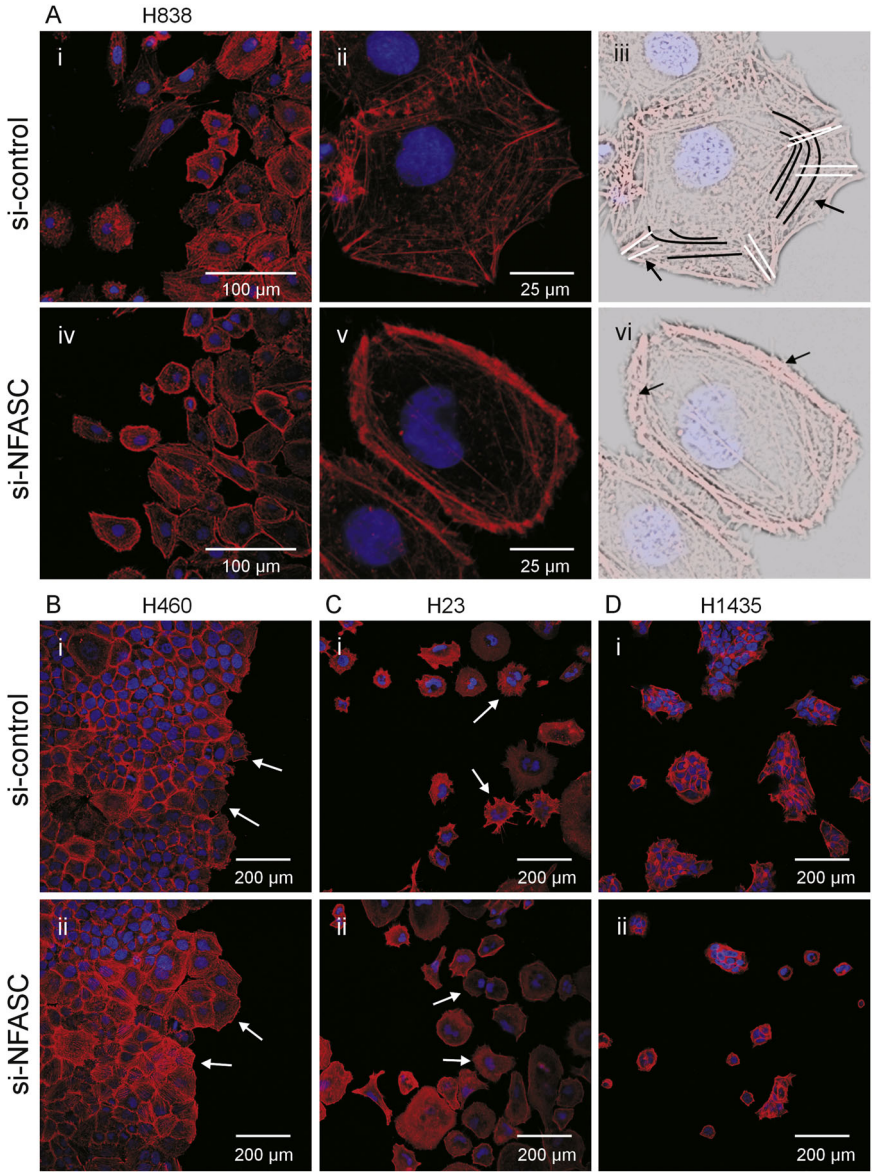

FIGURE 6 NFASC silencing altered the cytoskeletal organization of F-actin in migrating lung cancer cells. Rearrangements of F-actin (red) following NFASC silencing using siRNA were visualized by immunofluorescent microscopy in control cells (si-control) and in NFASC silenced cells (si-NFASC). Hoechst (blue) was used to counterstain cell nuclei. Images presented are representative of two or three conducted experiments with three replicates in each. (A) F-actin staining in migrating H838 cells; (i) and (ii) indicate si-control cells and (iv) and (v) indicate si-NFASC cells. (iii) and (vi) represent schematic illustrations to clarify changes in F-actin organization in control and NFASC silenced H838 cells. (iii) Arrows indicate transverse arches (black lines) and stress fibers (white lines). (vi) Arrows indicate cortical organized actin. (B) F-actin staining in migrating H460 cells; (i) and (ii) indicate si-control cells and si-NFASC cells, respectively. Arrows point to cells at the migrating cell front. (C) F-actin staining in migrating H23 cells; (i) and (ii) indicate si-control cells and si-NFASC cells, respectively. Arrows point to cell protrusions in migrating cells. (D) F-actin staining in H1435 cells on 100 ng/µL matrigel coating; (i) and (ii) indicate si-control cells and si-NFASC cells, respectively

types.[5,7,11,18–20,23,28] The role of NFASC in carcinogenesis remains, however, widely unexplored. We here show that *NFASC* copy number and expression are more frequently increased in NSCLC tumor tissues than in non-tumorous tissues. Amplifications of the *NFASC* gene have not previously been reported in lung cancer. However, copy number gain and increased expression of L1 have been demonstrated in breast cancer.[3] Moreover, increased L1 expression has been observed in various cancers including lung, glioma, ovarian, pancreatic, and colon carcinomas.[6–11] Our result showed that alterations in *NFASC* copy number were most common in adenocarcinoma. Interestingly, some of the patients showed *NFASC* copy number loss in the non-tumorous tissue but not in the paired tumor tissue. Thus, possibly, the amplification event itself is important for cancer development and progression. Furthermore, L1 expression is associated with poor survival in patients with several types of cancers, including lung cancer.[6,8,9,11,12,29] Our data may indicate that the effects of *NFASC* amplifications on lung cancer survival might be dependent on histology and need to be confirmed in larger studies.

Possible mechanisms for the role of NFASC in lung carcinogenesis were evaluated by NFASC silencing in H838, H460, H23, and H1435 cells. For screening purposes, the effects of NFASC silencing on the expression of 84 common lung cancer genes were analyzed in H838 cells. Silencing of the *NFASC* gene was associated with a significant reduction in the expression of CSF3, DUSP6, KRT14, CDKN1C, KRAS, and STAT1. Moreover, a moderate increase in the expression of RASSF1, FHIT, and AKT1, and a trend toward an increased expression of TERT and NFKB was observed in NFASC silenced cells. The most prominent effects of NFASC silencing in H838 cells were found on *CSF3* and *DUSP6* genes, which expressions were five- and twofold reduced following NFASC silencing in H838 cells. CSF3 is secreted by certain tumors, including NSCLC tumors, and has been found to regulate the actin cytoskeleton, adherent and tight junctions, and to increase cell motility. Moreover, CSF3 may modulate progression of solid tumors and elevated CSF3 expression levels are correlated with shorter survival in NSCLC.[30] DUSP6 regulates ERK1/2, which is involved in the phosphorylation of many proteins including transcription factors, receptors and cytoskeletal proteins.[31] Here, signaling pathways downstream of CSF3 and DUSP6, that is, ERK1/2 and STAT1, STAT3,[31,32] as well as p-AKT, which is a known target of L1 signaling, were studied. Both p-AKT and p-ERK levels were reduced following NFASC silencing, indicating that these signaling pathways might be of importance in understanding the effects of NFASC on NSCLC progression. pSTAT1 and pSTAT3 were not regulated following NFASC silencing in H838 cells. It should be noted that the involvement of these signaling events were not investigated in other lung cancer cell lines and results may not be generalized to all NSCLC cells and, thus, need further verification.

The gene array data suggest a possible involvement of NFASC in cellular processes such as growth and development, organization of cell compartments, localization, and response to stimuli in lung cancer progression. L1 has been indicated to have an important role in cancer cell growth and survival.[20] Increased expression of MKI67 was observed in the NFASC silenced H838 and H460 cells. However, no effects on cell number nor cell viability were observed after NFASC silencing in any of the four investigated lung cancer cell lines, indicating that NFASC likely does not exhibit a cell survival regulating role in NSCLC progression.

Rather, NFASC could affect lung cancer progression through the regulation of lung cancer cell motility and migration. L1 mediates cell-cell cohesion and functions as a chemoattractant in breast cancer cells.[18,19] Furthermore, CHL1 has also been suggested to have a regulatory role in motility and migration of cancer cells.[5] Here, decreased H838 cell adhesion to laminin and fibronectin surfaces was observed following NFASC silencing. Moreover, NFASC silenced H838, H460, and H23 lung cancer cells had a reduced migration rate compared with controls. The cell lines used in this study are derived from lung cancer tumors and metastasis of different stages and have different morphology and migration patterns. Our findings suggest that NFASC exhibits a role in fine-tuning of NSCLC cell migration. NFASC silencing also reduced the H838 cells' ability to invade into a solid matrix of matrigel. Key players of tumor cell invasion are matrix metalloproteinases (MMPs). However, we observed no regulation of the MMPs; MMP1, MMP9, and MMP12 analyzed in this study but cannot rule out action of other MMPs in the observed effect of NFASC on H838 cell invasion.

Further analysis of F-actin organization identified rearrangements of F-actin and changes in the lung cancer cells' morphology of migrating cells following NFASC silencing in NSCLC cells. A loss of transverse arcs and stress fibers was observed in NFASC silenced H838 cells compared with controls. Furthermore, NFASC silenced H838 cells had a higher abundance of cortically located actin filaments. Transverse arcs and stress fibers are contractile bundles that are differentiated by their orientation to the leading cell edge, with stress fibers aligned in the direction of migration and transverse arcs oriented perpendicularly.[33,34] The loss of such contractile bundle formation in NFASC silenced H838 cells could explain the observed reduction in the migration rate, and increased cortical actin may affect cell adhesion and migration. H460 cells migrated slowly into the induced wound through collective migration. In these cells, increased F-actin staining was observed only at the leading cell front in migrating NFASC silenced cells, but clear changes in F-actin organization were not observed. NFASC silencing in H23 cells seemed to reduce the number of long actin-based cell protrusions and silenced cells showed a more rounded morphology than control cells. Similarly, H1435 cells exhibited clear morphological changes on matrigel surface following NFASC silencing. H1435 control cells had a higher grade of confluency than silenced cells 48 h after seeding, however, as no effects on cell proliferation were observed, these changes are likely due to higher cell spreading in H1435 control cells. Indeed, NFASC silenced cells were more densely clustered and showed more intense F-actin staining than control cells. Together, these findings support a role of NFASC in the regulation of tumor cell motility through a regulation of the cells' actin filament formation and by alteration of cell morphology during migration.

In summary, increased *NFASC* copy number and gene expression in lung cancer tumors indicate a role of NFASC in lung cancer. We demonstrate a possible role of NFASC in the regulation of cytoskeletal organization and migration of lung cancer cells. NFASC does not seem to be involved in the regulation of cell proliferation, but rather, our data suggest a role of NFASC in the initiation and fine-tuning of NSCLC cell motility. Our findings suggest that one possible mechanism for the effects of NFASC on lung cancer cell migration may be through rearrangement of the actin cytoskeleton. Based on these results we suggest a role of NFASC in the regulation of lung cancer cell migration and metastasis. Further, larger studies are needed to evaluate the importance of NFASC signaling and to reconfirm possible effects of NFASC CNVs on survival and prognosis of *NSCLC* patients.

ACKNOWLEDGMENTS

Dr Lodve B. Stangeland (University of Bergen, Norway) is acknowledged for his kind contribution in collecting tissue samples. We are very grateful to Dr Øivind Skare for his assistance with statistical analysis. We also thank Ms Mayes Kasem, Ms Heidi Ødegaard Notø, Ms Rita Bæra, Mrs Tove Andreassen, and Mrs Elin Thorner Einarsdottir for excellent technical assistance.

CONFLICT OF INTERESTS

The authors declare no conflict of interests.

REFERENCES

1. Kriebel M, Wuchter J, Trinks S, Volkmer H. Neurofascin: a switch between neuronal plasticity and stability. *Int J Biochem Cell Biol*. 2012;44:694–697.
2. Herron Lissa R, Hill M, Davey F, Gunn-Moore Frank J. The intracellular interactions of the L1 family of cell adhesion molecules. *Biochem J*. 2009;419:519–531.
3. Valladares A, Hernández NG, Gómez FS, et al. Genetic expression profiles and chromosomal alterations in sporadic breast cancer in Mexican women. *Cancer Genet Cytogenet*. 2006;170:147–151.
4. Ludwig S, Ivanovich J, Graubert T, Goodfellow P. Copy number variants in early-onset-breast cancer. *Cancer Res*. 2011;71:P2-07-01.
5. He L-H, Ma Q, Shi Y-H, et al. CHL1 is involved in human breast tumorigenesis and progression. *Biochem Biophys Res Commun*. 2013;438:433–438.
6. Ben Q-W, Wang J-C, Liu J, et al. Positive expression of L1-CAM is associated with perineural invasion and poor outcome in pancreatic ductal adenocarcinoma. *Ann Surg Oncol*. 2010;17:2213–2221.
7. Gavert N, Conacci-Sorrell M, Gast D, et al. L1, a novel target of β-catenin signaling, transforms cells and is expressed at the invasive front of colon cancers. *J Cell Biol*. 2005;168:633–642.
8. Kaifi JT, Reichelt U, Quaas A, et al. L1 is associated with micrometastatic spread and poor outcome in colorectal cancer. *Mod Pathol*. 2007;20:1183–1190.
9. Tischler V, Pfeifer M, Hausladen S, et al. L1CAM protein expression is associated with poor prognosis in non-small cell lung cancer. *Mol Cancer*. 2011;10:127.
10. Tsuzuki T, Izumoto S, Ohnishi T, Hiraga S, Arita N, Hayakawa T. Neural cell adhesion molecule L1 in gliomas: correlation with TGF-beta and p53. *J Clin Pathol*. 1998;51:13–17.
11. Zecchini S, Bianchi M, Colombo N, et al. The differential role of L1 in ovarian carcinoma and normal ovarian surface epithelium. *Cancer Res*. 2008;68:1110–1118.
12. Chen D-l, Zeng Z-l, Yang J, et al. L1cam promotes tumor progression and metastasis and is an independent unfavorable prognostic factor in gastric cancer. *J Hematol Oncol*. 2013;6:43.
13. Siesser PF, Maness PF. L1 cell adhesion molecules as regulators of tumor cell invasiveness. *Cell Adh Migr*. 2009;3:275–277.
14. Kiefel H, Bondong S, Hazin J, et al. L1CAM: a major driver for tumor cell invasion and motility. *Cell Adh Migr*. 2012;6:374–384.
15. Raveh S, Gavert N, Ben-Ze'ev A. L1 cell adhesion molecule (L1CAM) in invasive tumors. *Cancer Lett*. 2009;282:137–145.
16. Wai Wong C, Dye DE, Coombe DR. The role of immunoglobulin superfamily cell adhesion molecules in cancer metastasis. *Int J Cell Biol*. 2012;2012:340296.
17. Silletti S, Yebra M, Perez B, Cirulli V, McMahon M, Montgomery AMP. Extracellular signal-regulated kinase (ERK)-dependent gene expression contributes to L1 cell adhesion molecule-dependent motility and invasion. *J Biol Chem*. 2004;279:28880–28888.
18. Shtutman M, Levina E, Ohouo P, Baig M, Roninson IB. Cell adhesion molecule L1 disrupts E-cadherin-containing adherens junctions and increases scattering and motility of MCF7 breast carcinoma cells. *Cancer Res*. 2006;66:11370–11380.
19. Li Y, Galileo DS. Soluble L1CAM promotes breast cancer cell adhesion and migration in vitro, but not invasion. *Cancer Cell Int*. 2010;10:34.
20. Bao S, Wu Q, Li Z, et al. Targeting cancer stem cells through L1CAM suppresses glioma growth. *Cancer Res*. 2008;68:6043–6048.
21. Knogler K, Grünberg J, Zimmermann K, et al. Copper-67 radioimmunotherapy and growth inhibition by anti-L1-cell adhesion molecule monoclonal antibodies in a therapy model of ovarian cancer metastasis. *Clin Cancer Res*. 2007;13:603–611.
22. Schafer H, Dieckmann C, Korniienko O, et al. Combined treatment of L1CAM antibodies and cytostatic drugs improve the therapeutic response of pancreatic and ovarian carcinoma. *Cancer Lett*. 2012;319:66–82.
23. Conacci-Sorrell ME, Ben-Yedidia T, Shtutman M, Feinstein E, Einat P, Ben-Ze'ev A. Nr-CAM is a target gene of the β-catenin/LEF-1 pathway in melanoma and colon cancer and its expression enhances motility and confers tumorigenesis. *Genes Dev*. 2002;16:2058–2072.
24. Górka B, Skubis-Zegadło J, Mikula M, Bardadin K, Paliczka E, Czarnocka B. NrCAM, a neuronal system cell-adhesion molecule, is induced in papillary thyroid carcinomas. *Br J Cancer*. 2007;97:531–538.
25. Lukashova-v.Zangen I, Kneitz S, Monoranu C-M, et al. Ependymoma gene expression profiles associated with histological subtype, proliferation, and patient survival. *Acta Neuropathol*. 2007;113:325–337.
26. Sehgal A, Boynton AL, Young RF, et al. Cell adhesion molecule Nr-CAM is over-expressed in human brain tumors. *Int J Cancer*. 1998;76:451–458.
27. Samulin Erdem J, Skaug V, Bakke P, Gulsvik A, Haugen A, Zienolddiny S. Mutations in TP53 increase the risk of SOX2 copy number alterations and silencing of TP53 reduces SOX2 expression in non-small cell lung cancer. *BMC Cancer*. 2016;16:28.
28. Ben Q, An WEI, Fei J, et al. Downregulation of L1CAM inhibits proliferation, invasion and arrests cell cycle progression in pancreatic cancer cells in vitro. *Exp Ther Med*. 2014;7:785–790.
29. Fogel M, Gutwein P, Mechtersheimer S, et al. L1 expression as a predictor of progression and survival in patients with uterine and ovarian carcinomas. *Lancet*. 2003;362:869–875.
30. Aliper AM, Frieden-Korovkina VP, Buzdin A, Roumiantsev SA, Zhavoronkov A. A role for G-CSF and GM-CSF in nonmyeloid cancers. *Cancer Med*. 2014;3:737–746.
31. Bermudez O, Pagès G, Gimond C. The dual-specificity MAP kinase phosphatases: critical roles in development and cancer. *Am J Physiol Cell Physiol*. 2010;299:C189–C202.
32. Kamezaki K, Shimoda K, Numata A, et al. Roles of stat3 and ERK in G-CSF signaling. *Stem cells*. 2005;23:252–263.
33. Heath JP. Behaviour and structure of the leading lamella in moving fibroblasts. I. Occurrence and centripetal movement of arc-shaped microfilament bundles beneath the dorsal cell surface. *J Cell Sci*. 1983;60:331–354.
34. Small JV, Rottner K, Kaverina I, Anderson KI. Assembling an actin cytoskeleton for cell attachment and movement. *Biochim Biophys Acta Mol Cell Res*. 1998;1404:271–281.

SUPPORTING INFORMATION

Additional Supporting Information may be found online in the supporting information tab for this article.

How to cite this article: Samulin Erdem J, Arnoldussen YJ, Skaug V, Haugen A, Zienolddiny S. Copy number variation, increased gene expression, and molecular mechanisms of neurofascin in lung cancer. *Molecular Carcinogenesis*. 2017; 56:2076–2085. https://doi.org/10.1002/mc.22664